JOURNAL OF GEOPHYSICAL RESEARCH, VOL. 104, NO. D16, PAGES 19,559–19,567, AUGUST 27, 1999

Improving first-order snow-related deficiencies in a regional climate model

Glen E. Liston, Roger A. Pielke Sr., and Ethan M. Greene
Department of Atmospheric Science, Colorado State University, Fort Collins

Abstract. A climate version of the Regional Atmospheric Modeling System (RAMS) is used to simulate snow-related land-atmosphere interactions in the Great Plains and Rocky Mountain regions of the United States. The availability of observed snow-distribution products allow snow-water-equivalent distribution data to be assimilated directly into the RAMS simulations. By performing two kinds of model integrations, one with and one without assimilating the snow-distribution observations, the differences between the model runs are used to highlight model deficiencies and limitations and thus identify areas of possible improvement in the atmospheric model. The need to simulate subgrid snow distributions is identified and addressed by implementing a snow submodel that accounts for subgrid variations in air temperature and precipitation. This subgrid snow model is found to significantly improve the model's simulation of snow-related processes.

1. Introduction

With its high albedo, low thermal conductivity, and considerable spatial and temporal variability, seasonal snow cover overlying land plays a key role in governing the Earth's global radiation balance; this balance is the primary driver of the Earth's atmospheric circulation system and associated climate. Of the various features that influence the surface radiation balance, the location and duration of snow cover comprise two of the most important seasonal variables. In the Northern Hemisphere the mean monthly land area covered by snow ranges from 7 to 40% during the annual cycle, making snow cover the most rapidly varying large-scale surface feature on Earth [*Hall*, 1988]. Snow-covered landscapes adjacent to bare-soil regions have been found to produce mesoscale wind circulations [*Johnson et al*., 1984], and snow cover also influences the dispersion of air pollution because of the more stable boundary layers over this cold surface [e.g., *Segal et al*., 1991a, b, c]. In addition to its role in governing atmospheric processes, the snow distribution plays a key role in controlling land-surface hydrologic processes, influencing early-season soil moisture and runoff [*U.S. Army Corps of Engineers*, 1956].

Realistically representing seasonal snow accumulation and depletion in regional and global atmospheric and hydrologic models is complex because key snow-related features possess considerable temporal and spatial variability. These differences also occur at scales below those resolved by the models. As an example of this variability, over the winter landscape in middle and high latitudes, the interactions between wind, vegetation, and topography produce snowcovers of nonuniform depth and density [e.g., *Liston and Sturm*, 1998]. In addition, orographically produced precipitation can display significant spatial variation in mountainous regions where topographic gradients are high [e.g., *Daly et al*., 1994; *Abbs and Pielke*, 1987; *Wesley and Pielke*, 1990; *Snook and Pielke*, 1995]. In light of the role that snow plays in influencing land and atmospheric processes, it is essential that local, regional, and global models used to simulate weather, climate, and hydrologic interactions be capable of accurately describing the seasonal-snow evolution. In past years, significant achievements have been made to better represent snow cover in climate models [*Verseghy*, 1991; *Lynch-Stieglitz*, 1994; *Marshall and Oglesby*, 1994], but current climate-model simulations of seasonal snow still do not adequately reproduce the observed snow distributions [e.g., *Foster et al*., 1996]. Typically, snow accumulation and melt in climate models are simulated by applying simple energy and mass balance accounting procedures [*Foster et al*., 1996]. These algorithms frequently neglect or oversimplify important physical processes, such as those associated with subgrid-scale temporal and spatial snow-distribution variability. To account for snow-distribution-related processes in weather, climate, and hydrologic models, we must first be able to simulate the snow distribution.

This paper addresses some of the reasons why snow distributions are misrepresented in regional and global atmospheric models and suggests possible enhancements to the models in order to correct the identified deficiencies. The model simulations are performed using a climate version of the Regional Atmospheric Modeling System (RAMS) which is capable of performing full annual integrations. The suggested enhancements are implemented in RAMS and used to demonstrate the improvement gained over the original model formulation.

Paper number 1999JD900055.
0148-0227/99/1999JD900055$09.00

2. Model Description

RAMS was developed at Colorado State University primarily to facilitate research into mesoscale and regional, cloud and land-surface atmospheric phenomena and interactions [*Tripoli and Cotton*, 1982; *Pielke et al*., 1992]. The model is fully three-dimensional; nonhydrostatic; includes telescoping, interactive nested grid capabilities [*Walko et al*., 1995]; supports various turbulence closure, short and longwave radiation, initialization, and boundary condition schemes; includes a land-surface energy balance submodel which accounts for vegetation, open water, and snow-related surface fluxes; and includes explicit cloud microphysical submodels describing liquid and ice processes related to clouds and precipitation. The references de-

scribing each of these RAMS components can be found in the work of *Pielke et al*. [1992].

The climate version of RAMS used in this study contains all of the above features, with the addition of several modifications designed to allow year-to-multiyear integrations. To meet the requirements of a regional model running at both weather and climate timescales, several modifications to the base modeling system were made, including the following: (1) sea surface temperatures and vegetation parameters are updated daily throughout each year; (2) a collection of routines which simulates grid-scale snow accumulation, snowmelt, and their effects on surface hydrology and surface energy exchanges are included; and (3) a relative-humidity-based precipitation scheme [*Cotton et al*., 1995] for long model runs was implemented. In this version of RAMS the snow model accounts for key features of the snow cover and its atmospheric and hydrologic interactions and feedbacks. The primary components of the snow model are as follows: (1) precipitation is assumed to fall as snow if the temperature of the lowest atmospheric model level is $\leq$0°C; (2) the snowpack is represented by one layer of constant density and thermal properties; (3) the albedo is modified as a function of snow depth (when shallow) and whether the snow is dry or melting; (4) the ground heat-flux computation is modified as a function of snow depth; (5) the surface roughness changes when snow is present; (6) the surface temperature is constrained to be $\leq$0°C when snow is present; (7) the available energy to melt snow is computed as part of the surface energy balance; and (8) snow meltwater is added to the soil-moisture store.

As an initial test of how the regional atmospheric model performs in simulating the snow distribution in both mountainous and prairie landscapes, RAMS was used in three independent simulations. The first simulation is one where no observed snow data were included in the model. This integration started September 1, 1995, when no snow was present in the domain and continued through June 30, 1996, when the majority of the snow cover had melted. The second simulation started January 26, 1996, where the observed snow distribution was used to define the snow initial conditions and then ran through June 30, 1996. The third simulation also ran from January 26 to June 30, 1996, but in this simulation, the observed snow distribution was assimilated into the model on any day that snow-distribution observations were available. This assimilation or updating methodology involved a simple replacement of the modeled snow distribution with that which was observed. This third run with the assimilated snow observations is considered the "truth" for the purposes of the following discussions and analyses of the model integrations. Effectively, this assimilation procedure increases the model snow depth to equal that which was observed on the observation dates. The resulting snow depth increase or decrease can influence the surface albedo, ground heat flux, surface roughness, surface temperature, and available melting energy; these are all addressed within the context of the model's surface energy and moisture balances. For the case of a snow depth increase, these changes are accounted for in the same way that would occur under conditions of a snow precipitation event. For a snow depth decrease, the extra snow is simply removed from the domain. These assimilation procedures can lead to moisture imbalances between the atmosphere and the land surface. For example, a snow depth increase from the updating procedure is not balanced by a removal of that equivalent moisture from the atmosphere. Another moisture imbalance will occur if the model melts the snow cover too fast and is then updated by more snow, which must also eventually melt. In this case, too much meltwater is produced, leading to overestimates of snowmelt energy, soil moisture, and runoff. In spite of these limitations, updating the snow distribution when observations are available allows additional insights into how the model is representing the general snow distribution and evolution. Specifically, it provides a physically based and time continuous evolution of the snow cover that allows an analysis of the model's behavior (e.g., a comparison of accumulation and ablation quantities) between the snow-distribution updates throughout the snow season.

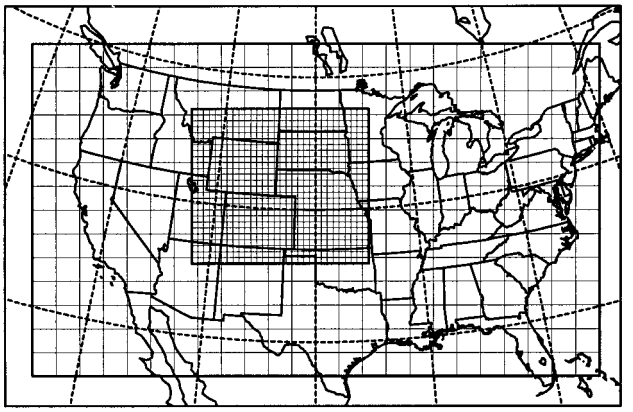

Figure 1. Regional Atmospheric Modeling System (RAMS) simulation domain and grid configuration. Coarse and fine-grid intervals are 200 km and 50 km, respectively.

The model domain and grid configurations are given in Figure 1, where a 200 km grid covers almost the entire conterminous United States, and a 50 km nested grid covers Kansas, Nebraska, South Dakota, Wyoming, Colorado, and parts of the regions surrounding those states. The model is driven with six-hourly lateral boundary conditions defined using National Centers for Environmental Prediction (NCEP) atmospheric analyses [*Kalnay et al*., 1996].

3. Observed Snow Distributions

Observed snow-distribution data provide the key snow-related input and validation products used in the model simulations. Snow-water-equivalent depth distributions were generated which provide complete coverage of the conterminous United States. This was done by merging two data sets: the National Operational Hydrologic Remote Sensing Center (NOHRSC) snow-water-equivalent depth data and the National Climatic Data Center (NCDC) summary-of-the-day (SOD) meteorological-station snow depth data. The NOHRSC data cover the western United States (west of ~100°W longitude) on a 30 arc-sec latitude-longitude grid (~1-km) and are derived from a variety of remote sensing and ground-based observations, including the mountain-based United States Natural Resources Conservation Service SNOTEL (snow telemetry) observations [*Carroll*, 1997]. They are available approximately twice per week during the late-winter through early-summer months. The 1995–1996 winter was chosen for these simulations because there are a greater number of NOHRSC data sets than in previous winters. The 10-year monthly-average SOD snow-depth record, averaged over the 50 km grid

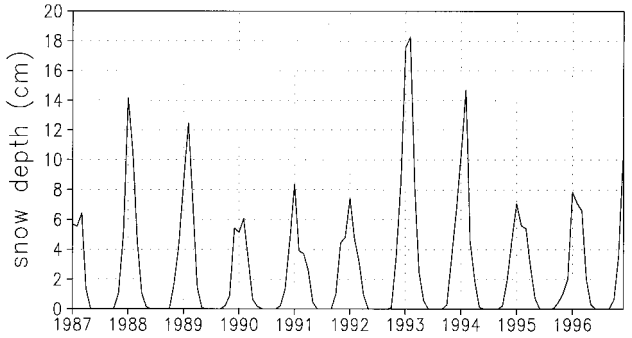

Figure 2. Monthly-average summary-of-the-day snow depth climatology, averaged over the 50 km grid in Figure 1.

in Figure 1, indicates that the 1995–1996 winter is representative of the typical snow depth climatology for this region (Figure 2). The NOHRSC data sets are particularly valuable for the current study because of the relatively high resolution snow-distribution representation in the mountainous regions of the model domain. The SOD observations are available throughout the year and have a daily temporal coverage that includes ~3800 stations distributed across the United States.

The availability of NOHRSC data was used to define the temporal frequency of the merged snow-water-equivalent distribution data sets. On these dates the SOD station data were gridded to a 5 km grid using an objective analysis scheme [*Cressman*, 1959]. The resulting snow depth distributions were then converted to snow-water-equivalent distributions using the snow-classification distribution of *Sturm et al*. [1995], where the snow density used for each of the snow classes is given in Table 1. The NOHRSC data were then gridded to the same 5 km grid as that used for the SOD data. Comparison of the SOD snow-water-equivalent distributions with the NOHRSC data, for the coincident prairie regions of the domain, showed the snow density correction of the SOD snow depth data to be acceptable. The two data sets were then merged to provide spatially continuous, 5 km coverage over the conterminous United States. Because of the broader collection of data sources used in the NOHRSC data sets, the NOHRSC data are used wherever both data sets are coincident. Efforts to use the available NOHRSC and SOD information to generate a daily record were unsuccessful; in mountainous regions the generally-valley locations of the SOD data make it difficult to reconstruct the mountain snow distributions represented in the NOHRSC data sets. The temporal coverage of the resulting data set is given in Figure 3. Examples of the resulting gridded snow-data fields, for a Colorado subdomain, are given in Figure 4 for the dates of January 26, April 16, May 10, and June 5, 1996. These 5 km data were then regridded to the 200 and 50 km RAMS grids for use in the model simulations. Examples of the resulting 50 km gridded fields are given in Figure 5 for the same dates as those given in Figure 4.

Table 1. Snow Densities Used to Convert Snow Depth to Snow-Water-Equivalent Depth Using Snow-Classification Distribution of *Sturm et al*. [1995]

Snow Classification	Snow Density, kg m^{-3}
Tundra	280
Taiga	225
Alpine	250
Prairie	250
Maritime	300
Ephemeral	350

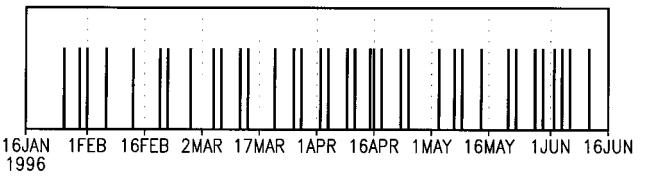

Figure 3. Temporal availability (indicated by the bars) of the conterminous United States, 5-km-gridded snow-water-equivalent observational data.

4. Model Simulations

For the purpose of analyzing the three RAMS simulations we will focus on the same Colorado subdomain as that given in Figure 4. For this region the domain-averaged snow-water-equivalent depth distributions for the three simulations are given in Figure 6. For the September through June simulation, with no assimilation of the observed snow distributions, the model underrepresents the observed snow volume by approximately one half, and the snow-free date is approximately one month early. For the case of only providing the snow initial conditions, the snowpack buildup from spring storms is underrepresented, and the snow-free date is approximately two weeks earlier than for the case where the approximately twice-weekly snow observations are used to update the snow distribution as the simulation progresses in time. The temporal snow-distribution evolution for the Colorado subdomain is

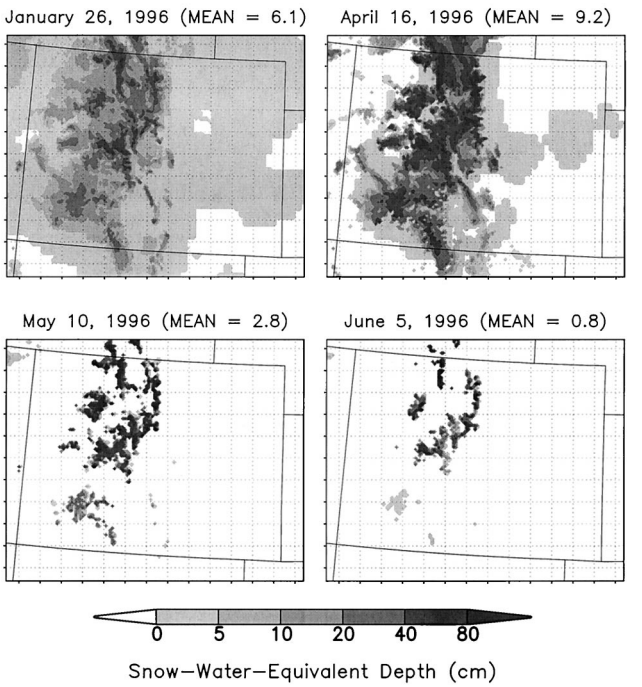

Figure 4. Example 5-km-gridded snow-water-equivalent observations for a Colorado subdomain of the model domain given in Figure 1.

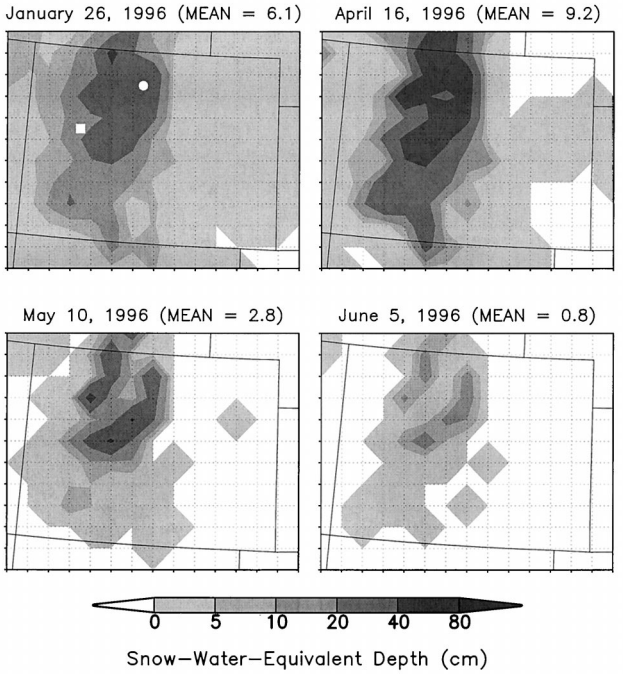

Figure 5. Observed snow-water-equivalent distributions given in Figure 4 when regridded to the RAMS 50 km grid. The white markers in the January 26 panel identify the grid cells discussed as part of Figures 8, 9, 10, and 12.

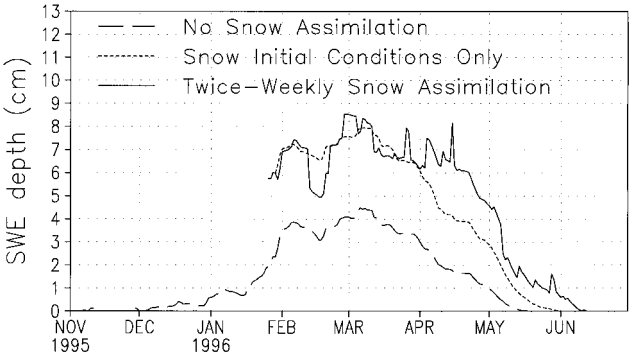

Figure 6. Domain-averaged snow-water-equivalent depth distributions for the Colorado subdomain given in Figure 4 for three RAMS simulations: (1) no assimilation of the observed snow-water-equivalent data (simulation running from September 1, 1995 to June 30, 1996), (2) the snow initial conditions given by the January 26, 1996, observed snow-water-equivalent distribution (simulation running from January 16 to June 30, 1996), and (3) observed snow-water-equivalent distributions assimilated when available, as defined in Figure 3 (simulation running from January 16 to June 30, 1996).

given in Figure 7. Figure 7, when compared with the observed distribution in Figure 5, also highlights the low snow-depth bias in the model and the premature snow-free date.

To help understand the reasons why the model is misrepresenting the snow accumulation and ablation within the model domain, Figure 8 describes the temporal evolution of snow-water-equivalent depth for the model grid cells identified by the white markers in the January 26 panel of Figure 5. Figure 8 displays the snow evolution for the cases where only the initial snow distribution was supplied and where the modeled snow distributions were updated when observations were available. For the circle-marker grid cell, the snow depth for the initial-condition-only curve underrepresents the snow depth by approximately one half, and the snow-free date is approximately one month early. For the square-marker grid cell, the initial-condition-only curve overestimates the snow depth. The two primary reasons for these misrepresentations of snow depth evolution can be tied directly to the model's precipitation and air temperature representation, and these are related, at least in part, to the model's relatively smooth topography. These factors are highlighted by comparison of the topographic representations on the 5 km and 50 km grids given in Figure 9. Also included in Figure 9 are the same grid-cell markers given in Figure 5. The observed 5 km topography displays two factors that are important in the analysis of the model's snow depth underrepresentation. First, the model's smooth representation of topography does not allow adequate simulation of the orographic-lifting processes associated with winter precipitation in mountainous terrain. As a consequence, the winter snow accumulation can be significantly underestimated. Second, the smooth model topography can be lower (higher) than some regions described by the 5 km topographic representation (Figure 9a). The circle- and square-marker locations have been chosen to correspond to grid cells that are higher and lower in the 5 km topography than the 50 km topography, respectively. In the model this produces higher (lower) surface air temperatures than those found in the higher (lower) elevations of the 5 km topography. These higher (lower) air temperatures lead to increased (decreased) melt rates and the possibility of precipitation events occurring as rain (snow) instead of snow (rain). Figure 10 displays the modeled and observed precipitation corresponding to the Figure 8 grid

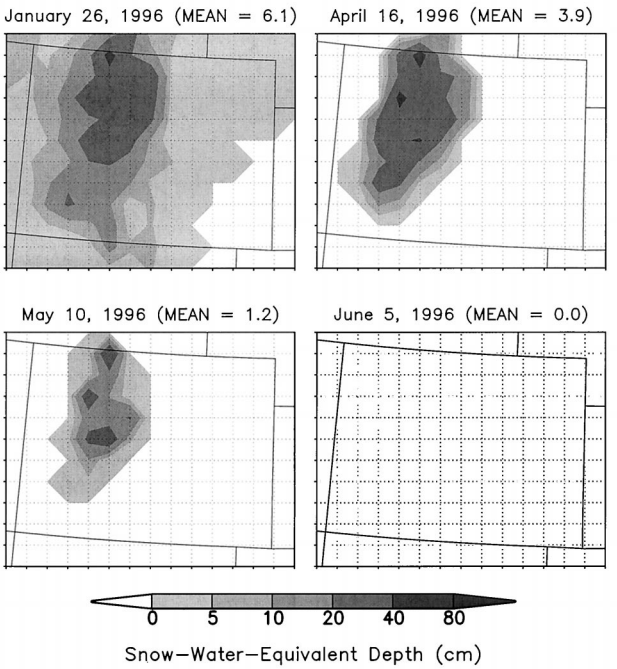

Figure 7. RAMS simulation of the temporal evolution of snow-water-equivalent distribution for the Colorado subdomain for the case where only the January 26, 1996, observed snow-water-equivalent distribution was provided as initial conditions.

cells. In the model the circle-marker grid cell underestimates the precipitation, and the square-marker grid cell overestimates the precipitation. Figure 11 displays the corresponding air temperature evolutions, where the modeled circle-marker grid cell is found to closely follow the observations, and the modeled square-marker grid cell significantly underestimates the air temperature. As further support of this analysis and the close relationship between topography and snow distribution, the observed 5-km snow distribution in Figure 4 closely follows the pattern of the observed topography at the same resolution (Figure 9a).

The underrepresentation of snow depth and the premature snow-free date illustrated in Figure 8 have important consequences for the surface energy and moisture balances. Figure 12 displays the temporal evolution of daily-averaged runoff for the grid cells, represented by the white markers in Figures 5 and 9, for the cases where only the snow initial conditions were supplied and where the snow distributions were updated when observations were available. As a further comparison of these two model simulations, the differences between key atmospheric and surface energy and moisture variables are provided in Table 2. This table also highlights the monthly evolution of the different variables. As previously noted, the procedure of repeatedly updating the snow distribution could lead to a misrepresentation of the surface energy and moisture fluxes. As an example of this, the runoff values, cited in Table 2, might be unreasonably high, but unfortunately, we have no way of quantifying any possible misrepresentation.

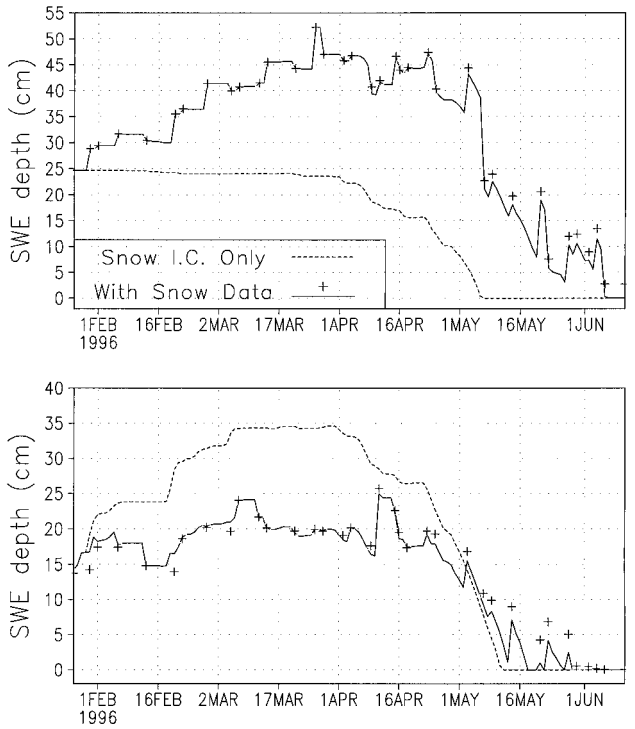

Figure 8. RAMS temporal evolution of snow-water-equivalent depth at the model grid cells identified by the white markers in the January 26 panel of Figure 5 for the two simulations where the snow observations were only used to define the snow initial conditions and where the snow observations (the plus markers) were used to continuously update the model's snow distribution. The top panel corresponds to the round marker, and the bottom panel corresponds to the square marker.

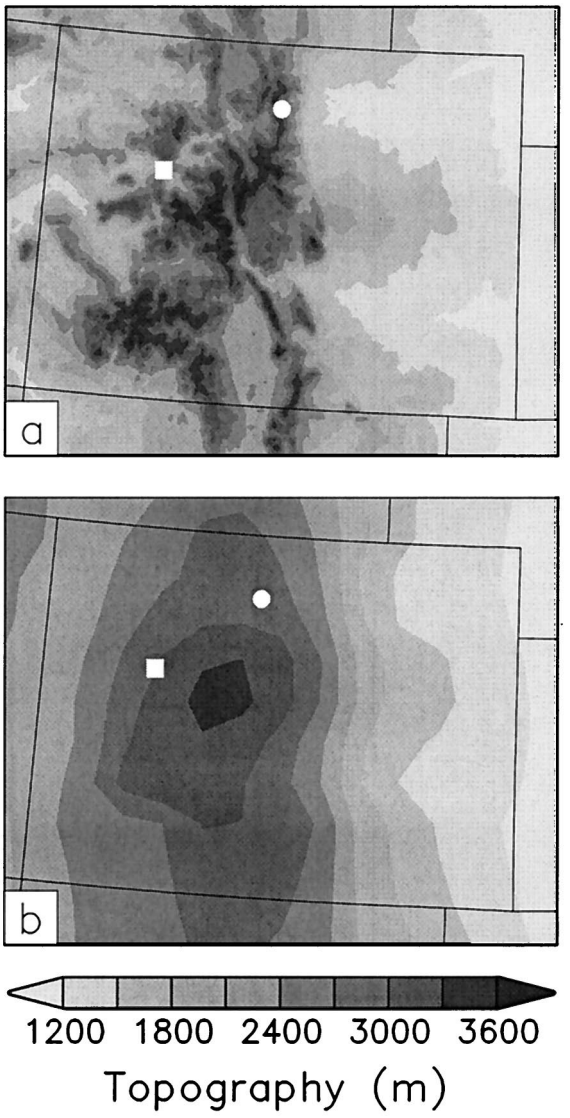

Figure 9. Topographic representations: (a) 5 km and (b) 50 km for the Colorado subdomain. The white markers identify the same grid-cell locations as the those given in Figure 5.

The existence or nonexistence of snowcover affects nearly all components of the surface energy balance, including the outgoing shortwave and longwave radiation, sensible, latent, and conductive heat fluxes, and the energy flux associated with melting. Consequently, the snow-free date is an important factor that directly impacts land-atmosphere interactions and feedbacks. In addition, both snow volume and melt rate strongly influence snowmelt-runoff volume and timing, thus influencing key components of the land-surface hydrologic cycle.

5. Subgrid Snow Model

The previous model-simulation analysis suggests that there are two primary sub-grid-scale features that need to be accounted for in the regional atmospheric model to realistically simulate the seasonal snow cover evolution in mountainous terrain: the orographically induced winter-precipitation distribution and the sub-grid-scale temperature distribution and its influence on melt rates. In what follows we present a subgrid

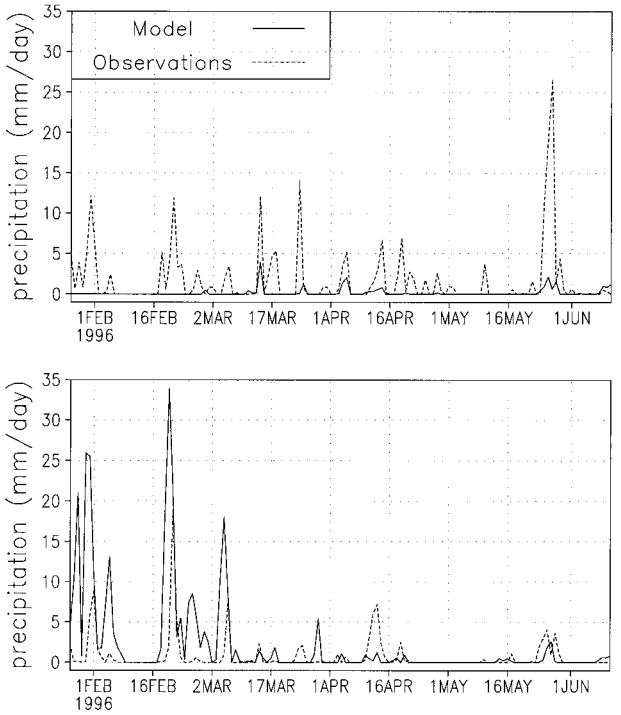

Figure 10. Observed and modeled precipitation for the model grid cell identified by (top) the circle and (bottom) the square markers in the January 26 panel of Figure 5.

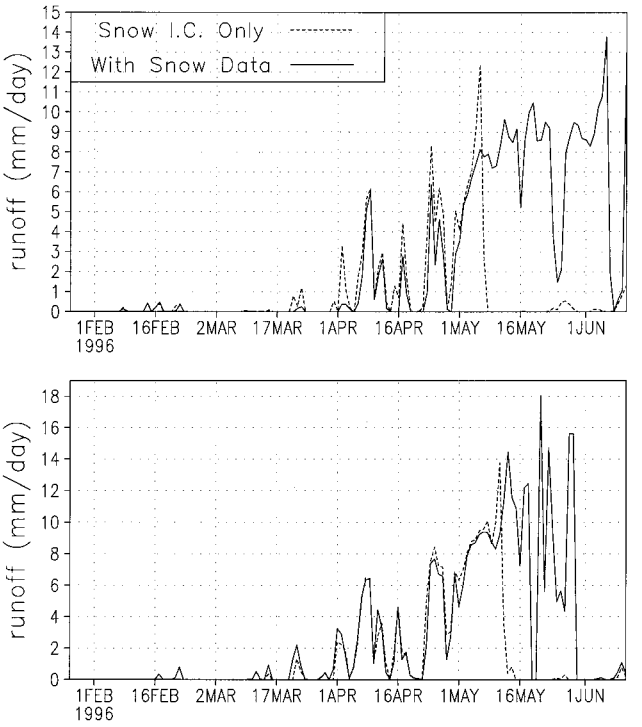

Figure 12. Temporal evolution of runoff for the RAMS grid cells represented by (top) the circle and (bottom) the square markers in Figures 5 and 12 for the two simulations identified in Figure 8.

snow model that accounts for these two features and discuss the results of simulations using this new model.

The general premise behind the following approach is that a higher-resolution snow submodel can be used to describe the snow-related processes and that this snow submodel can receive its dominant forcing from the larger-scale regional atmospheric model. The snow submodel is essentially the same mass- and energy-balance snow model used in RAMS, but it has been configured to operate over a coincident higher-resolution grid. In this application the specific snow-related features to be addressed are the subgrid air temperature and precipitation distributions, and they will be described using simple functions tied directly to the subgrid topographic distribution. The snow submodel is cast over the same domain as the 50 km RAMS grid (Figure 1) but is configured as a 5 km grid, thus leading to 100, 5 km grid cells coincident with each 50 km RAMS grid cell. The snow submodel receives the following input from the RAMS 50 km grid: incoming shortwave and longwave radiation, precipitation, wind speed, relative humidity, and air temperature. All of these variables, except air temperature and precipitation, are considered to be uniform over each of the 100, 5 km grid cells that are coincident with the associated 50 km RAMS grid cell. In its current simple formulation the subgrid snow distributions do not influence the calculation of other land-surface processes such as soil moisture and the subsequent interactions and feedbacks with the atmosphere. We are currently developing a subgrid snow parameterization that will account for the more complete and physically realistic two-way coupling between the atmosphere and snow-covered and snow-free land surfaces, but those developments have not been implemented as part of the snow submodel discussed herein.

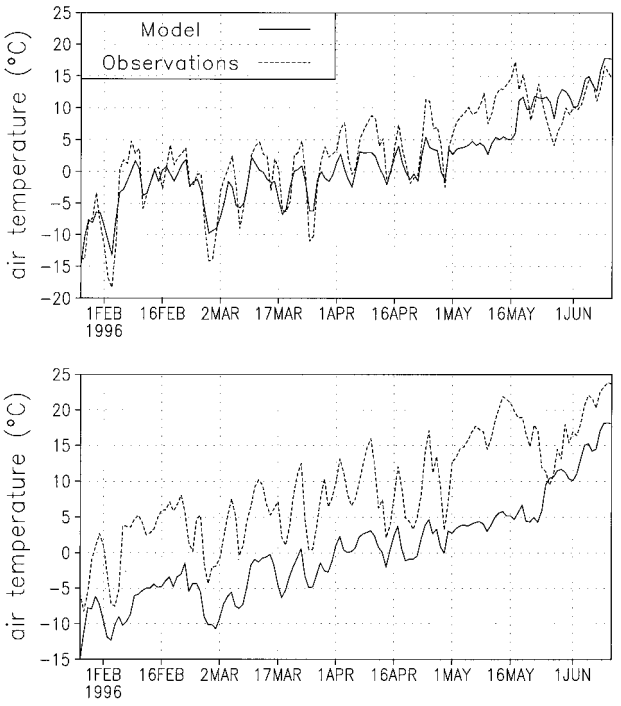

Figure 11. Observed and modeled screen-height air temperature for the model grid cell identified by (top) the circle and (bottom) the square markers in the January 26 panel of Figure 5.

To define the subgrid air temperature field, over each of the 100, 5 km grid subdomains, the coincident 50 km RAMS temperature is distributed using the linear relationship

Table 2. Atmospheric and Surface Variables, Spatially Averaged Over the Western Half of Colorado for Each Month of Second and Third Model Simulations (As Defined in Figure 6)

	February	March	April	May	June
Snow-water-equivalent depth, cm	−0.1	0.3	5.2	3.1	0.4
Snow-covered fraction (0–1)	−0.01	−0.02	0.12	0.15	0.05
Two-meter air temperature, °C	0.5	0.2	−1.0	−1.6	−1.2
Precipitation, mm month^{-1}	−1.0	−0.4	0.3	0.7	2.1
Runoff, mm month^{-1}	3.9	5.1	18.2	47.5	23.6
Sensible heat flux, W m^{-2}	0.4	−1.3	−12.0	−25.5	−16.3
Latent heat flux, W m^{-2}	0.8	2.8	4.1	17.3	13.3
Melt energy, W m^{-2}	0.8	0.9	3.8	10.1	4.7

Shown are differences between the simulation with twice-weekly snow assimilation and the simulation with snow initial conditions only. Before performing the difference, the heat flux variables were defined as having positive values for fluxes toward the atmosphere.

$$T_{hr} = T_{lr} + \Gamma \delta z \tag{1}$$

where T_{hr} is the air temperature for the high-resolution grid cell, T_{lr} is the air temperature of the low-resolution (RAMS) grid cell, Γ is the atmospheric lapse rate defined to be −6.5°C km^{-1}, and δz is the difference between the high-resolution topographic height H_{hr} and the low-resolution topographic height H_{lr} (i.e., $\delta z = H_{hr} - H_{lr}$).

In a similar manner the low-resolution RAMS precipitation, P_{lr}, is converted to the precipitation over the relatively high resolution grid, P_{hr}, according to the relationship

$$P_{hr} = \begin{cases} P_{lr}(1 + \beta \cdot \delta z); & H_{hr} > H_{lr} \\ P_{lr}; & H_{hr} \le H_{lr} \end{cases} \tag{2}$$

where β is an empirical coefficient assumed to be 8.0 km^{-1}, a number that was found to provide a qualitative best fit to the observed snow-distribution data. This orographic precipitation parameterization has the effect of enhancing precipitation at submodel elevations that are higher than the elevations given by the 50 km grid. While we recognize that this methodology is deficient in numerous regards, its purpose in this application is to demonstrate that some form of subgrid winter orographic precipitation scheme is required to realistically simulate the seasonal snow evolution within atmospheric models using relatively coarse grids. Given this general objective, the relationship given by equation (2) has been found to be adequate. Additional support for the application of simple precipitation and elevation relationships can be found from numerous observational studies that find generally linear increases in precipitation with increasing elevation [see *Daly et al.*, 1994; *Thornton et al.*, 1997; *Baron et al.*, 1998].

Implementation of equations (1) and (2) provides the high-resolution atmospheric-forcing inputs to the snow submodel and leads to the snow distributions given in Figure 13. In this simulation the observed snow-distribution initial conditions have been provided, and no additional snow observations have been assimilated. When comparing Figure 13 to the observed distributions of Figure 4, and the 50 km RAMS simulation given in Figure 7, the subgrid snow model has significantly improved the snow-distribution simulation. Figures 4, 7, and 13 highlight both improvements in the spatial snow cover representation and the temporal snow cover evolution. The relative influence of equations (1) and (2) is highlighted in Figure 14, where these equations have been applied independently and then together. Applying the precipitation equation enhances the snow accumulation in the upper elevations of the subgrid topography. Applying the temperature equation reduces the melting in the upper elevations while enhancing it in lower elevations. The combined effect is to produce a deeper snowpack from February to late April.

6. Conclusions

Implementing a simple subgrid snow-distribution representation in a regional atmospheric model has produced improved spatial and temporal distributions of snow-water-equivalent depth, when compared with the outputs of the model running with a 50 km grid. The subgrid methodology uses a 5 km grid covering the same domain as the 50 km grid and performs the same energy- and mass-balance accounting over the 5 km grid used in the atmospheric model. This finer-resolution snow

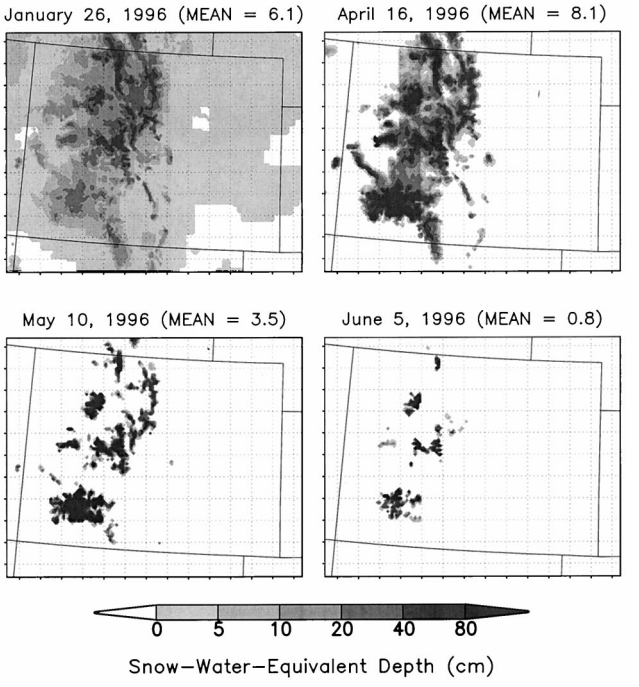

Figure 13. Temporal evolution of snow-water-equivalent distribution simulated by the higher-resolution snow submodel, when driven by RAMS-produced atmospheric forcing that was spatially redistributed according to equations (1) and (2).

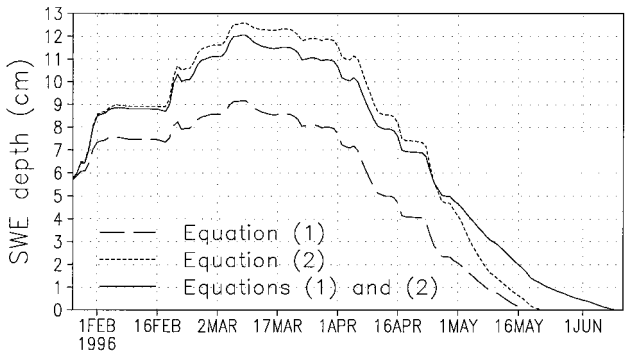

Figure 14. Domain-averaged snow-water-equivalent depth distributions for the Colorado subdomain given in Figure 4 for three simulations using the higher-resolution snow submodel: (1) application of the temperature parameterization (equation (1) and (2)) application of the precipitation parameterization (equation (2) and (3)) application of both the temperature and the precipitation parameterizations.

submodel receives inputs of incoming shortwave and longwave radiation, wind speed, and relative humidity at the same resolution as the atmospheric model while applying subgrid air temperature and precipitation functions that distribute the two variables according to the subgrid topographic variation. Accounting for the subgrid precipitation distribution influences the snow accumulation patterns, and accounting for the subgrid temperature distribution affects the snow ablation. In contrast to summer convective-precipitation systems, which do not generally remain anchored over the higher elevations, the spatial distribution of winter precipitation is more directly tied to the topographic distribution. This suggests that precipitation-topographic relationships can play an important role in defining the sub-grid-scale snow distributions within the context of atmospheric models running at regional and global scales.

Potential improvements to this methodology include also distributing the relative humidity, incoming longwave radiation, and wind speed across the higher-resolution topography. As another improvement, the lapse rate used to distribute the air temperature could be obtained from the atmospheric model and thus vary spatially and temporally instead of being constant. Shortwave radiation striking the Earth's surface is known to vary according to slope and aspect, and this could be accounted for in the subgrid model by following the methodology outlined by *Pielke* [1984]. Improved computational efficiency could be achieved by considering subgrid elevation bands instead of the fine-grid approach adopted here.

The natural topography generally has much greater variability than that represented by regional and larger-scale atmospheric models. To begin to remedy this deficiency, a simple empirical subgrid parameterization of orographic precipitation was introduced to distribute the model-produced moisture over the subgrid topography. As an alternative to this simple formulation, other statistical [e.g., *Hevesi et al*., 1992a, b; *Daly et al*., 1994; *Thornton et al*., 1997] and physically based [e.g., *Barros and Lettenmaier*, 1993a, b; *Leung and Ghan*, 1995] methods could be used.

This study has shown that the relatively coarse resolution of the regional atmospheric model does not allow an accurate representation of processes related to the snow distribution in complex terrain. This has important implications regarding the model simulation of atmospheric and hydrologic processes, because the presence of snow has such a large impact on the surface energy budget and because the snow distribution in mountainous terrain is frequently quite variable on scales much finer than those represented by the atmospheric model. As an example, comparing the June 5, 1996, observed 5 km snow distribution (Figure 4) with the same data cast on the 50 km grid (Figure 5) shows that the snow-covered area, while preserving the same snow volume, can be significantly misrepresented. This, in turn, affects the albedo and other components of the surface energy balance. Representing the subgrid snow distribution is also important from a land-surface hydrology perspective. Again, considering the June 5, 1996, observed 5 km (Figure 4) and 50 km (Figure 5) snow distributions, the meltwater-production patterns in the two representations are significantly influenced by the spatial snow distribution (not shown). This, in turn, affects the soil-moisture distribution and runoff characteristics. These factors indicate that a realistic representation of the seasonal snow evolution, and its associated interactions with land-surface hydrologic processes, will also require a subgrid representation of soil moisture and runoff.

Acknowledgments. This work was supported by NOAA grant NA67RJ0152, NASA grant NAG5-4760, and NPS contracts CA 1268-2-9004, COLR-R92-0204, and CEGR-R92-0193.

References

Abbs, D. J., and R. A. Pielke, Numerical simulations of orographic effects on NE Colorado snowstorms, *Meteorol. Atmos. Phys*., *37*, 1–10, 1987.

Baron, J. S., M. D. Hartman, T. G. F. Kittel, L. E. Band, D. S. Ojima, and R. B. Lammers, Effects of land cover, water redistribution, and temperature on ecosystem processes in the South Platte Basin, *Ecol. Appl*., *8*(4), 1037–1051, 1998.

Barros, A. P., and D. P. Lettenmaier, Dynamic modeling of orographically induced precipitation, *Rev. Geophys*., *32*, 265–284, 1993a.

Barros, A. P., and D. P. Lettenmaier, Dynamic modeling of the spatial distribution of precipitation in remote mountainous areas, *Mon. Weather Rev*., *121*, 1195–1214, 1993b.

Carroll, T. R., Integrated observations and processing of snow cover data in the NWS hydrology program, in *Proceedings of the 77th of the AMS Annual Meeting on Integrated Observing Systems*, pp. 180–183, Am. Meteorol. Soc., Boston, Mass., 1997.

Cotton, W. R., J. F. Weaver, and B. A. Beitler, An unusual summertime downslope wind event in Fort Collins, Colorado, on 3 July 1993, *Weather Forecast*., *10*, 786–797, 1995.

Cressman, G. P., An operational objective analysis system, *Mon. Weather Rev*., *87*, 367–374, 1959.

Daly, C., R. P. Neilson, and D. L. Phillips, A statistical-topographic model for mapping climatological precipitation over mountainous terrain, *J. Appl. Meteorol*., *33*, 140–158, 1994.

Foster, J., G. Liston, R. Koster, R. Essery, H. Behr, L. Dumenil, D. Verseghy, S. Thompson, D. Pollard, and J. Cohen, Snow cover and snow mass intercomparisons of general circulation models and remotely sensed datasets, *J. Clim*., *9*, 409–426, 1996.

Hall, D. K., Assessment of polar climate change using satellite technology, *Rev. Geophys*., *26*(1), 26–39, 1988.

Hevesi, J. A., J. D. Istok, and A. L. Flint, Precipitation estimation in mountainous terrain using multivariate geostatistics, I, Structural analysis, *J. Appl. Meteorol*., *31*, 661–676, 1992a.

Hevesi, J. A., A. L. Flint, and J. D. Istok, Precipitation estimation in mountainous terrain using multivariate geostatistics, II, Isohyetal maps, *J. Appl. Meteorol*., *31*, 667–688, 1992b.

Johnson, R. H., G. S. Young, and J. J. Toth, Mesoscale weather effects of variable snow cover over northeast Colorado, *Mon. Weather Rev*., *112*, 1141–1152, 1984.

Kalnay, E., et al., The NMC/NCAR reanalysis project, *Bull. Am. Meteorol. Soc*., *77*, 437–471, 1996.

Leung, R. L., and S. J. Ghan, A subgrid parameterization of orographic precipitation, *Theor. Appl. Climatol*., *52*, 95–118, 1995.

Liston, G. E., and M. Sturm, A snow-transport model for complex terrain, *J. Glaciol*., *44*(148), 498–516, 1998.

Lynch-Stieglitz, M., The development and validation of a simple snow model for the GISS GCM, *J. Clim*., *7*, 1842–1855, 1994.

Marshell, S., and R. J. Oglesby, An improved snow hydrology for GCMs, 1, Snow cover fraction, albedo, grain size, and age, *Clim. Dyn*., *10*, 21–37, 1994.

Pielke, R. A., *Mesoscale Meteorological Modeling*, 612 pp., Academic, San Diego, 1984.

Pielke, R. A., et al., A comprehensive meteorological modeling system—RAMS, *Meteorol. Atmos. Phys*., *49*, 69–91, 1992.

Segal, M., J. R. Garratt, R. A. Pielke, and Z. Ye, Scaling and numerical model evaluation of snow-cover effects on the generation and modification of daytime mesoscale circulations, *J. Atmos. Sci*., *48*, 1024–1042, 1991a.

Segal, M., J. H. Cramer, R. A. Pielke, J. R. Garratt, and P. Hildebrand, Observational evaluation of the snow-breeze, *Mon. Weather Rev*., *119*, 412–424, 1991b.

Segal, M., J. R. Garratt, R. A. Pielke, P. Hildebrand, F. A. Rogers, and J. Cramer, On the impact of snow cover on daytime pollution dispersion, *Atmos. Environ*., *25*(B), 177–192, 1991c.

Snook, J. S., and R. A. Pielke, Diagnosing a Colorado heavy snow event with a nonhydrostatic mesoscale numerical model structured for operational use, *Weather Forecast*., *10*, 261–285, 1995.

Sturm, M., J. Holmgren, and G. E. Liston, A seasonal snow cover classification system for local to global applications, *J. Clim*., *8*(5), 1261–1283, 1995.

Thornton, P. E., S. W. Running, and M. A. White, Generating surfaces of daily meteorological variables over large regions of complex terrain, *J. Hydrol*., *190*, 214–251, 1997.

Tripoli, G. J., and W. R. Cotton, The Colorado State University three-dimensional cloud/mesoscale model—1982, I, General theoretical framework and sensitivity experiments, *J. Rech. Atmos*., *16*, 185–220, 1982.

U.S. Army Corps of Engineers, *Snow Hydrology, Summary Report of the Snow Investigations*, 433 pp., Portland, Oregon, U.S. Govt. Print. Off., Washington, D. C., 1956.

Walko, R. L., C. J. Tremback, R. A. Pielke, and W. R. Cotton, An interactive nesting algorithm for stretched grids and variable nesting ratios, *J. Appl. Meteorol*., *34*, 994–999, 1995.

Wesley, D. A., and R. A. Pielke, Observations of blocking-induced convergence zones and effects on precipitation in complex terrain, *Atmos. Res*., *25*, 235–276, 1990.

Verseghy, D. L., CLASS—A Canadian land surface scheme for GCMs, I, Soil model, *Int. J. Climatol*., *11*, 111–133, 1991.

E. M. Greene, G. E. Liston, and R. A. Pielke Sr., Department of Atmospheric Science, Colorado State University, Fort Collins, CO 80523-1371. (liston@iceberg.atmos.colostate.edu)

(Received July 25, 1998; revised December 8, 1998;
accepted January 26, 1999.)